

Precision alignment of integrated optics in surface electrode ion traps for quantum information processing

Amber L. Young^{*a}, Jeffery D. Hunker^a, A. Robert Ellis^b, Daniel L. Stick^a, Sally Samora^a, Joel R. Wendt^a

^aSandia National Laboratories, P.O. Box 5800, Albuquerque, NM, USA 87111-1082; ^bArborlight, Ann Arbor, MI, USA 48109

ABSTRACT

The integration of optics for efficient light delivery and the collection of fluorescence from trapped ions in surface electrode ion traps is a key component to achieving scalability for quantum information processing. Diffractive optical elements (DOEs) present a promising approach as compared to bulk optics because of their small physical profile and their flexibility in tailoring the optical wavefront. The precise alignment of the optics for coupling fluorescence to and from the ions, however, poses a particular challenge. Excitation and manipulation of the ions requires a high degree of optical access, significantly restricting the area available for mounting components. The ion traps, DOEs, and other components are compact, constraining the manipulation of various elements. For efficient fluorescence collection from the ions the DOE must be have a large numerical aperture (NA), which results in greater sensitivity to misalignment. The ion traps are sensitive devices, a mechanical approach to alignment such as contacting the trap and using precision motors to back-off a set distance not only cannot achieve the desired alignment precision, but risks damage to the ion trap.

We have developed a non-contact precision optical alignment technique. We use line foci produced by off-axis linear Fresnel zone plates (FZPs) projected on alignment targets etched in the top metal layer of the ion trap and demonstrate micron-level alignment accuracy.

Keywords: micro-optic integration, off-axis Fresnel zone plates, optical alignment, non-contact alignment, hybrid microsystems, surface electrode ion trap, diffractive optics

1. INTRODUCTION

The integration of micro-optics in hybrid microsystems enables greater efficiency in light manipulation, and, perhaps more importantly, is essential to the development of scalable technologies. Ion-based quantum information processing is an important application for micro-optic integration in which the small, integrated, format is an enabling technology for building the large arrays of trapped ion qubits, essential in considering the future of ion-based quantum communications [1-5]. Whether bulk optics or integrated optics are incorporated, their alignment with respect to the ion location must be both accurate and precise. This task is made more difficult by the aggressive design of the lenses. Large NAs to collect from a greater portion of the 4π steradians the ions are radiating into means smaller diffraction limited spot sizes, often less than 1 micron. The challenge is to align the focal spot of these lenses that have high sensitivity to misalignment to the location of the ions with maximum precision and accuracy in order to maximize efficiency in addressing the ion or in fluorescence collection from the ion. To further confine the task requirements, the challenge must be met without negatively impacting the trap or optics wafers. Avoiding mechanical stress and surface contact that might cause surface damage are important. The aligned components must interconnect with a system that does not interfere with geometric constraints, and can tolerate environmental demands including temperature cycling, and vacuum environments. The solution must maintain tight alignment requirements through assembly, thermal cycling, pressure cycling, and mechanical stresses.

We have developed a non-contact optical alignment technique inspired by Ayliffe, et al [6] that uses off-axis linear FZPs to achieve sub-micron alignment accuracy between a micro-optical collection lens etched in a fused silica substrate and a surface electrode ion trap 500 microns away. The use of wedged aluminum posts and a carefully selected choice of UHV-compatible epoxy enabled final hybrid assemblies with repeatable micron-level alignment precision and accuracy. We demonstrate that alignment is maintained through epoxy cure, thermal cycling, and the vacuum environment.

2. OFF-AXIS LINEAR FRESNEL ZONE PLATES

A Fresnel zone plate takes advantage of the Fresnel zones of an optical surface, which define regions of the wavefront passing through the element that will constructively and destructively interfere along the optical axis. The radial transition points for these alternating zones are defined by Equation 1

$$r_n = \sqrt{n\lambda f + \frac{n^2\lambda^2}{4}} \quad (1)$$

Where r_n is the radius of zone n , λ is the wavelength of the propagating field, f is the focal length of the lens and n is the zone number, counting from the center of the lens out to the edge [7]. Blocking the destructively interfering zones (as in an amplitude zone plate), leaves only the zones that interfere constructively to focus the wavefront. An alternative to blocking the zones that would otherwise yield destructive interference is to modify the phase delay experienced by the wavefront in these zones. The phase delay can be designed such that the portions of the wavefront passing through these segments will also contribute to constructive interference at the focus. An FZP with transition points in only one lateral direction, as opposed to circular features defined by radial transition points, is a linear FZP, illustrated in Figure 1. Linear features focus the light in one direction, but not the orthogonal direction, producing line foci.

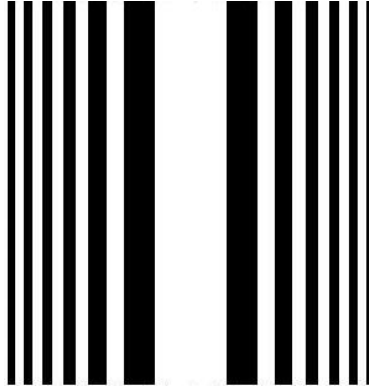


Figure 1: Illustration of the lateral transition points in a linear FZP. The alternating zones may be transparent and opaque as in an amplitude FZP. Alternatively, a phase delay imposed on the wavefront in the dark zones in the figure, for example, may be designed such that the wavefronts from those regions constructively interfere with the transparent zones and contribute to the focal spot. Linear features, as shown here, focus light only in the direction normal to the long direction of the features, producing line foci whose diffraction limited width is defined by the width of the outermost zones of the FZP and whose length matches the long direction of the linear features.

In an FZP functioning as a lens that focuses incoming wavefronts, the area of each zone is the same. Near the center, the zones are wide, but near the edges of the structure, at larger radial distances, the width of the zones is narrow. It is these outer zones that determine the maximum resolution of the FZP, the size of the diffraction limited spot. An off-axis FZP is an off-axis segment of a standard FZP. It has the same focal length and zone radii relative to the “center,” though the central region is not a part of the fabricated design. The advantages of an off-axis element include a smaller footprint, since only the outer portion of the parent element is used, and a smaller diffraction limited spot is formed than for the

same size on-axis element. The trade-off is a loss in efficiency, as the wider central zones of an FZP, which are not fabricated in an off-axis design, make the largest contribution to the energy in the focal spot. However, for use in an optical alignment application, high efficiency is not necessary.

For example, consider a case in which we are aligning a fused silica substrate containing a lens to a second substrate 1 mm away and we are limited to FZPs on the fused silica substrate 500 microns long. Assuming a traditional FZP with a central plateau at the center and collimated illumination at 500 nm, the diffraction limited spot size has a 2.5 micron diameter. Using Equation 1, we find the width of the outermost zone is 1.0 microns. This width is attainable using contact printing and is nowhere near the limits of electron beam fabrication capabilities. Suppose, instead, we want to design for a desired alignment precision and choose a diffraction limited spot size of 1 micron diameter. This requires an NA of 0.61, which corresponds, at 1 mm away, to an equivalent element diameter of 1.5 mm, 3 times larger than our allotted space for a 500 micron element. We can, however, stick to the 500 micron limit by taking just a portion of the large element and use only the outer 250 micron ring of a circular FZP. In a linear FZP, this amounts to two rectangular segments, each 250 microns wide, symmetric about the center of the would-be 1.5 mm element, see Figure 2 for illustration. The two mirror-image segments are not necessary, one could take just one half, but together, they contribute to a brighter line focus on the target. By extracting these 250 micron wide portions, the same diffraction limited spot diameter of 1 micron formed by the full 1.5 mm wide element is maintained but the total width (now divided in two segments) is limited to just 500 microns and the FZP does not occupy additional valuable real estate on the optics chip in achieving the smaller diffracted line width. The small diffraction limited spot size enables greater alignment precision. While electron beam (e-beam) lithography is now required to fabricate the FZP instead of contact printing, we are nowhere near fabrication limited (for this element, the width of the outermost zone is 0.41 microns). The compromise in extracting only the outer section of the full FZP is in efficiency. The large central plateau and wider zones near the center of the element have the largest contribution to the intensity of the diffracted spot. For this application, however, this is a judicious trade-off as high efficiency is not necessary, one only requires sufficient throughput to see the spot (or line) to execute the alignment.

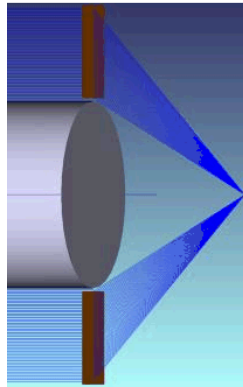


Figure 2: Zemax ray trace of the beam paths through off-axis FZPs. Assume collimated light passes through the fused silica substrate and is incident on the off-axis zone plates on the back side. Each diffracts the light and focuses the beam to the same location as if the full on-axis parent zone plate were there. In our design there is an aperture between the two off-axis FZPs. To prevent stray (undiffracted) light from obfuscating the focal lines, an obscuration is aligned over the center aperture.

There is another advantage to this geometry for off-axis linear FZPs in which two spatially separated segments of a larger parent FZP project narrow line foci on a target. The gap between the two off-axis FZP portions allows for an aperture for observation of the line foci. We are using the line foci projected by the off-axis FZPs to optically align two planes, the plane of the diffractive lens used for fluorescence collection, and the plane of the ion trap; the configuration is illustrated in Figure 3. The spacing between the two planes is too narrow to allow observation from the sides and the

two planes themselves are opaque (the fused silica substrate is coated with gold); the only available option for observation is intentional apertures in the gold coating on the fused silica.

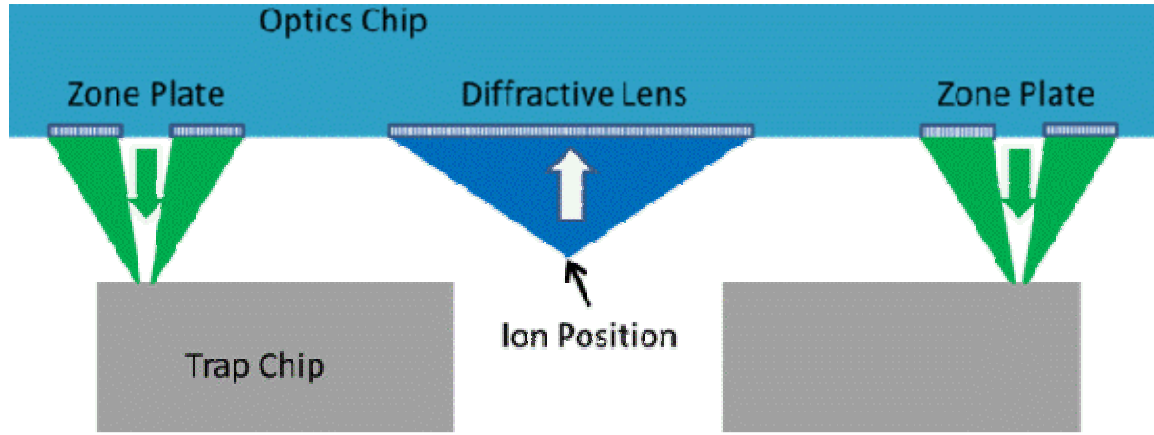


Figure 3: Schematic of fused silica substrate containing DOE and off-axis FZPs aligned over the surface electrode ion trap. The zone plates focus line foci onto alignment rulers on the surface of the ion trap. The diffractive lens collects fluorescence from the ion, above the surface of the trap.

3. ALIGNMENT TARGETS

In order to use the line foci of the off-axis linear FZPs for alignment, there must be targets to align to on the ion trap surface. Alignment targets are etched in the top metal layer of the trap, directly below each aperture between pairs of FZPs. Prudent design of the targets allows the targets to facilitate the alignment process, allows the identification of the correct alignment position, and enables quantification of alignment error. A portion of the alignment targets we designed are shown in the optical microscope image in Figure 4. The alignment rulers are designed with 1 micron wide lines and spaces. The center line is longer to indicate it as the center. The lines that are targeted for alignment are symmetrically displaced from center and, like the center line, are longer for easy identification. In addition, the outer ends of the lines are wider and step in from 5 microns wide at the ends, to 3 microns, to 1 micron through the center. The space on either side of the target lines is wider, 2 microns, to help distinguish the target lines. These features are designed to serve as guides to walk the line foci toward the ideal alignment position.

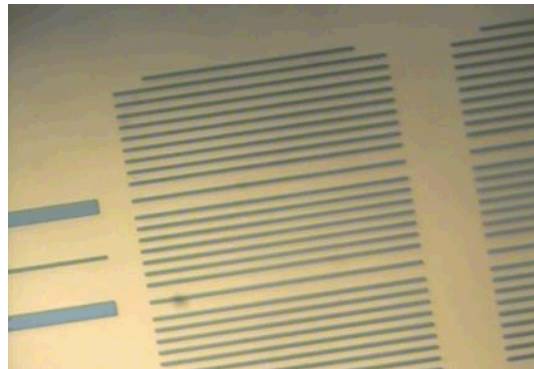


Figure 4: Alignment targets etched in the gold on the surface of the ion trap. Lines and spaces are 1 micron wide and 200 microns long (with a break through the center). The center line and the alignment targets on either side of center are longer for easy identification. The target alignment marks have segments that are 5 microns, 3 microns, and 1 micron wide, moving in from the ends, to help walk the line foci along the marks of the alignment ruler into their aligned position.

In order to cover all six degrees of freedom in the alignment process, three sets of line foci and their corresponding alignment targets are required. We include additional sets to ensure three good pairs in the case of fabrication errors. The four sets of FZPs and alignment rulers are laid out on their respective wafers in two sets of orthogonal pairs as shown in the wafer layout in Figure 5. The cartoon in Figure 6 illustrates the use of the line foci projected on the alignment targets to align the two planes in all six degrees of freedom. The diagonal paths of the pairs of beams as they come to focus between the off-axis FZPs and the alignment targets means there are two z-locations where the two beams fall on the alignment targets displaced from center in the alignment ruler. Moving back and forth between the two positions by adjusting the spacing of the two wafers ensures the correct side of the beam crossing is used. Lateral shift of the beams at the correct spacing directly translates to lateral misalignment of the two planes. A difference in spacing between the pair of line foci on one alignment ruler as compared to another indicates tilt error. Iterating between rotational and translational motions, perfect alignment with all four pairs of line foci centered on their corresponding alignment targets, is quickly achieved.

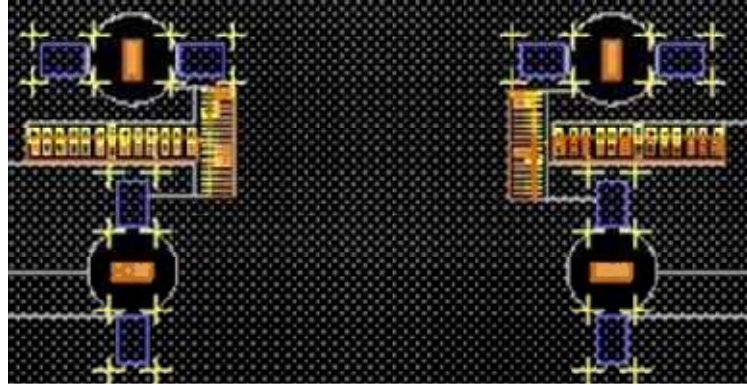


Figure 5: Layout of the fused silica wafer indicating the orientation of the four sets of off-axis zone plates (purple). Two produce horizontal foci, two produce vertical foci. The alignment targets in the center of each aperture (gold), are shown for illustration, but are fabricated in the surface of the ion trap, not in the fused silica.

Figure 7 shows a cartoon of the basic alignment set-up. The ion trap is locked in place in a ZIF socket while the fused silica optics wafer is mounted in an aluminum arm that can move in all six degrees of freedom. A beamsplitter mounted above the optics wafer allow illumination of the FZPs with a well-collimated green diode laser from one direction and observation through the apertures of the line foci projected on the alignment targets using a microscope objective and Navitar imaging system. With this set-up we are able to repeatedly accomplish alignment precision at the limit of the

system's capability, which is limited by the line width of the line foci and width of the alignment marks, where the latter is largely dictated by fabrication limits.

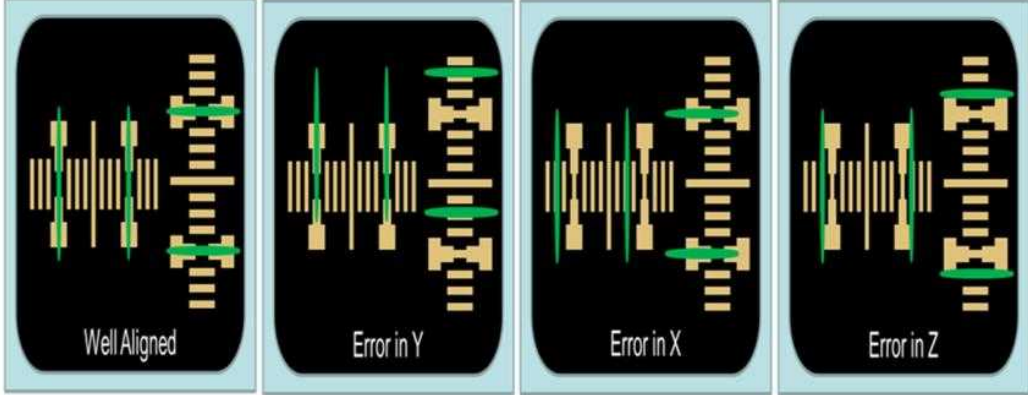


Figure 6: Cartoon illustrating the use of the alignment targets with the green line foci incident on the alignment rulers.

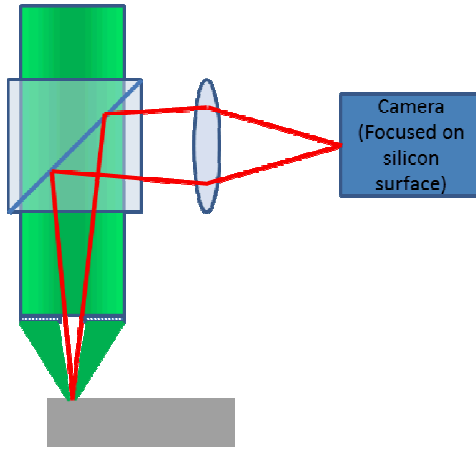


Figure 7: Set-up for the alignment process. The trap chip is immobilized (grey) and the optics wafer is mounted in a removable aluminum arm that can move in all six degrees of freedom to maneuver the optics chip into place over the trap. The beamsplitter allows illumination of the FZPs by a well-collimated green diode laser and observation of the line foci on the alignment rulers on the trap surface through the apertures using a microscope objective and Navitar imaging system.

4. BONDING ALIGNED COMPONENTS

The greater challenge once the two planes are well-aligned is bonding the two planes in place. The mechanical structure and epoxy used must be able to maintain the tight alignment tolerances while also meeting all other system requirements, including temperature cycling and vacuum compatibility. In this iteration we used micro-EDM machined wedged aluminum posts with grooves on the underside, shown in

Figure 8. The wedge allowed us to slide the posts into place from the side after alignment; the grooves improve wicking of the epoxy. After substantial testing, Masterbond EP21TCHT-1 was selected as the best epoxy for the application, meeting UHV compatibility, temperature, and strength requirements, and experimentally demonstrated to maintain alignment best. The bonding process began with carefully applying epoxy to the bonding pad on the trap package, setting an aluminum post in the epoxy and sliding it against the edge of the fused silica wafer. Once all four posts are in place, epoxy is carefully applied in the wedge between the post and fused silica. Throughout the process the alignment of the two planes is actively monitored and micro-adjustments can be made to the alignment if necessary, though the

motion controllers otherwise lock the Newport LTA-HL and LTA-HS actuators in place. After epoxy is applied, the alignment is actively monitored for up to 3 hours, though we found no micro-adjustments were needed after 30-45 minutes. The epoxy is then allowed to cure at room temperature for 72 hours, followed by a final cure at 70 C for 10 hours, where the oven is ramped up to 70 C from room temperature over the course of an hour, there is a 10 hour soak and the temperature is ramped down again over an hour. Finally, to demonstrate the success of the mounting and bonding solution, the device is baked at 150 C for 36 hours (temperature is slowly ramped before and after).

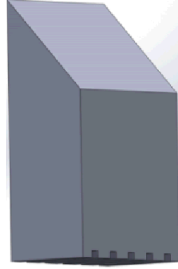


Figure 8: Micro-EDM fabricated wedged aluminum post with grooves in the base. Used to bond the fused silica optics wafer to the trap chip.

One of the many benefits of this non-contact alignment approach is that it enables quantification of the alignment position with respect to optimal alignment. After the final bake the difference from the ideal position is measured, the results are in Table 1. The most sensitive direction for alignment is transverse to the trap; any offset present parallel to the trap or vertically from the trap can be compensated. For this reason, the larger shift suffered by the first device along the trap line is inconsequential. The transverse shift for that same trap may be as much as 3 microns, but in the other two devices was significantly improved. The primary difference in these cases is that alignment was not actively monitored during epoxy cure in the first device. Making the micro-adjustments that may be necessary in the first minutes of epoxy cure is clearly beneficial.

	Device 1 (microns)	Device 2 (microns)	Device 3 (microns)
Offset along trap line	4.8 – 6.5	0.8 – 1.2	0.2 – 2.2
Offset transverse to trap	0.8 – 3.0	0.2 – 1.8	0.0 – 0.8
Vertical shift	1.7 – 3.7	0.2 – 3.9	0.0 – 2.6

Table 1: Final alignment positions for three devices.

5. CONCLUSION

While this non-contact optical alignment approach for hybrid microsystems proved highly successful, exceeding our goal to align the optics wafer to the trap to within 2.5 microns, there is room for improvement. The greatest need for improvement is in the bonding of the optics wafer to the trap package. A bonding geometry that does not over-constrain the movement, as is the case with the four point attachment is important and a mechanical assembly that maintains alignment in the most critical dimensions should be considered. A design employing flexures that restrict movement in the critical transverse direction is an important next step. Furthermore, additional consideration should be given to the application of epoxy, using such existing tools as metered micro-dispensing pens that are able to carefully control the amount of epoxy applied, thereby ensuring matching bond sizes to reduce strain introduced in the system during epoxy cure due to variations in bond size.

There is also room for improvement in the alignment process itself. The components are currently be aligned manually and this can be accomplished fairly quickly; however, it would not be difficult to automate the process. Computer vision algorithms are sufficiently advanced that it is not a far reach to allow software to find the centroid of the line foci, calculate the required shifts based on the offsets of the lines on each of the alignment rulers and command the motion controllers already in use to maneuver the two components into position. A computer vision approach to alignment could also take advantage of finer features in the alignment rulers and smaller diffraction limited line foci widths to achieve more precise alignment, though the greater limitations at the moment is maintaining alignment once achieved with an appropriate mounting assembly.

ACKNOWLEDGEMENT

Sandia National Laboratories is a multi-program laboratory managed and operated by Sandia Corporation, a wholly owned subsidiary of Lockheed Martin Corporation, for the U.S. Department of Energy's National Nuclear Security Administration under contract DE-AC04-94AL85000.

REFERENCES

- [1] Cruz-Cabrera, A. A., Kemme, S. A., Wendt, J. R., Kielpinski, D., Streed, E. W., Carter, T. R., Samora, S., "High efficiency DOEs at large diffraction angles for quantum information and computing architectures," Proc. SPIE 6482, 648209 (2007).
- [2] Kim, J., Kim, C., "Integrated optical approach to trapped ion quantum computation," Quant. Inf. Comput. 9(2), 181-202 (2009).
- [3] Brady, G. R., Ellis, A. R., Moehring, D. L., Stick, D., Highstrete, C., Fortier, K. M., Blain, M. G., Haltli, R. A., Cruz-Cabrera, A. A., Briggs, R. D., Wendt, J. R., Carter, T. R., Samora, S., Kemme, S. A., "Integration of fluorescence collection optics with a microfabricated surface electrode ion trap," Applied Physics B 103(4), 801-808 (2011).
- [4] Merrill, J. T., Volin, C., Landgren, D., Amini, J. M., Wright, K., S. Charles D., Pai, C-S, Hayden, H., Killian, T., Faircloth, D., Brown, K. R., Harter, A. W., Slusher, R. E., "Demonstration of integrated microscale optics in surface-electrode ion traps," New Journal of Physics 12(10), 103005 (2011).
- [5] Streed, E. W., Norton, B. G., Jechow, A., Weinhold, T. J., Kielpinski, D., "Imaging trapped ions with a microfabricated lens for quantum information processing," Physical Review Letters 106(1), 010502-1 – 010502-4 (2011).
- [6] Ayliffe, M. H., Châteauneuf, M., Rolston, D. R., Kirk, A. G., and Plant, D. V., "Six-Degrees-of-Freedom Alignment of Two-Dimensional Array Components by Use of Off-Axis Linear Fresnel Zone Plates," Applied Optics 40(35), 6515-6526 (2001).
- [7] Reference any optics textbook. See for example: Hecht, E., [Optics], Addison Wesley, San Francisco, 490-497 (2002).